Miniaturization of Electromagnetic Bandgap (EBG) Structures with High-permeability Magnetic Metal Sheet

Yoshitaka Toyota, Kengo Iokibe, Ryuji Koga
Department of Communication Network Engineering,
Okayama University, Okayama, Japan
Email: toyota@cne.okayama-u.ac.jp

Arif Ege Engin, Tae Hong Kim, Madhavan Swaminathan
Packaging Research Center/
School of Electrical and Computer Engineering,
Georgia Institute of Technology, Georgia, USA
Email: madhavan.swaminathan@ece.gatech.edu

***Abstract*—Electromagnetic bandgap (EBG) structures in a pair of parallel planes are quite effective for suppressing simultaneous switching noise, but they are too large to be applied to compact electronic devices. To miniaturize the EBG structures, we investigated an approach to interpose a high-permeability magnetic metal sheet between the parallel planes. The experimental results show that high permeability of the sheet shifts the stopband towards lower frequencies. This suggests that such sheets contribute to the miniaturization of the EBG structures. In addition, it is demonstrated that the imaginary part of the permeability can expand the stopband.**

I. Introduction

Since digital and RF/analog circuits in recent mixed-signal systems are densely packed, electromagnetic interference (EMI) is currently a critical performance issue. To solve this issue, it is essential to isolate sensitive RF/analog signals from digital noise, and the electromagnetic bandgap (EBG) structure is one candidate to achieve this.

To isolate RF/analog and digital blocks electrically, the EBG structure is more effective than a separated-plane structure [1] since it prevents the propagation of electromagnetic waves within a certain frequency range, that is, achieving a stopband. Examples of planar EBG structures are depicted in Fig. 1, and they provide excellent isolation of more than 60 dB [2], [3]. The planar EBG structures require no additional vias, which are necessary in EBG structures with a high impedance surface (HIS) [4], [5].

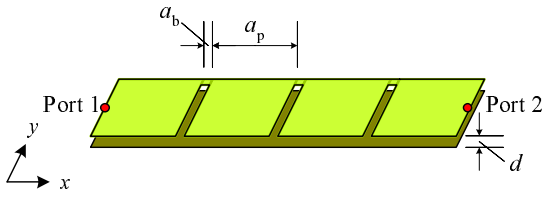

(a) 1-D EBG with a 4×1 lattice geometry.

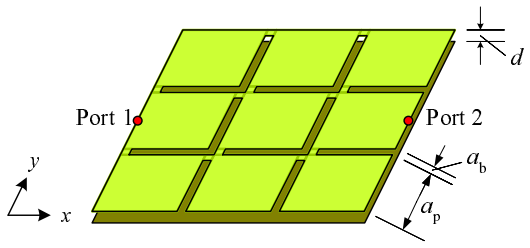

(b) 2-D EBG with a 3×3 lattice geometry.

Fig. 1. Examples of planar EBG lattices combining large square patches with small square branches in a PCB power/ground pair.

The EBG structure can be easily designed in a power/ground plane pair of a printed circuit board (PCB). Therefore, the standard PCB fabrication technique is easily applicable, which is a cost-effective solution. The planar EBG structure shown in Fig. 1 is a lattice with large metal patches and small metal branches connecting two large adjacent patches, and it has two variations: a one-dimensional (1-D) lattice (Fig. 1(a)) and a two-dimensional (2-D) lattice (Fig. 1(b)) formed in a power/ground pair. This paper deals only with patches and branches that are square in shape. The EBG lattice may be applied to either the power plane or the ground plane depending on the design.

To meet the general demand for more compact wireless devices at the frequency of interest, it is desirable to achieve the stopband caused by the EBG structure with patches that are as small as possible. However, a smaller patch makes the stopband frequency higher since the patch dimensions of this EBG structure determine the lower edge frequency of the stopband.

To shrink the dimensions with a high isolation at the frequency of interest, the authors studied two approaches [6]: introduction of narrow slits into the patch in the geometry, and application of high dielectric constant in the material. As a result, each approach was found to contribute to reducing the size of the EBG structure. Moreover, applying both approaches simultaneously made it possible to achieve an EBG structure in which the entire size was less than 20 mm per side and with sufficient isolation of the stopband around 2 GHz.

This paper discusses a third approach to miniaturize the EBG structure further: application of a high-permeability magnetic metal sheet with complex magnetic permeability to a pair of parallel planes in a PCB. The use of the magnetic metal sheet for miniaturization is novel as far as the authors know.

1-4244-1350-8/07/$25.00 ©2007 IEEE

It is expected that the use of this magnetic metal sheet will not only reduce the dimensions but also expand the stopband. This is because the large real part of the relative permeability contributes to reducing the size of the EBG structure. Also, the imaginary part of the relative permeability works to absorb electromagnetic waves.

II. Miniaturization of EBG Structure

A. The Concept of Miniaturization

The EBG structure shown in Fig. 1 has passbands and stopbands that alternate with frequency. At lower frequencies, the EBG structure can be considered to be a distributed LC network that works as a low-pass filter, because the large patches are predominantly capacitive, whereas the small patches are predominantly inductive. At higher frequencies, on the other hand, series and parallel resonances of the large patches occur. This paper focuses on the fundamental stopband following the lowest passband.

With a focus on miniaturizing the dimensions of the EBG structure, this paper directs attention to the lower edge frequency of the fundamental stopband. The frequency can be roughly estimated. Around frequencies of the fundamental stopband, the EBG structure is regarded as a distributed LC network, and hence, an EBG unit cell can be expressed as a network with series inductor L and shunt capacitor C. According to filter theory [7], a cutoff frequency of a low-pass filter with a ladder LC network is inversely proportional to $\sqrt{LC}$. The cutoff frequency corresponds to the lower edge frequency of the fundamental stopband in the EBG structure because its unit cell can be roughly regarded as a network consisting of series inductance L and shunt capacitance C at lower frequencies, as described above.

As seen in the above relationship with the cutoff frequency of a low-pass filter, a simple size reduction decreases the patch capacitance of C. Thereby, the lower edge frequency of the EBG stopband moves towards the higher frequencies. The miniaturization of the EBG structure must be compatible with a sufficient isolation at the frequency of interest. Therefore, two options can be selected: (A) to compensate the decrease in C by increasing L; or (B) to maintain the value of C under the patch size reduction.

The effect of these options is confirmed by observing a stopband shift towards the lower frequencies. The stopband shift indicates that the dimensions have been reduced without changing the frequency of interest.

B. Two Approaches Investigated So Far

The authors in [6] investigated two effective approaches to shrink the EBG dimensions with high isolation at the frequency of interest: applying narrow slits to the patch in the geometry; and applying high dielectric constant in the material.

The first approach associated with option (A) increases branch inductance L. Figure 2 shows an EBG unit cell with two narrow slits that have width w_s on the patch side. The length of the slit is defined as $L_\mathrm{r}a_\mathrm{p}$ using a slit-length ratio L_r that takes a value between 0 and 1. The narrow slits help lengthen the side of the square branch with side a_b in order to increase the inductance of the branch. In [6], the optimum value of the slit-length ratio L_r is concluded to be 50%, because branches that are too long will degrade isolation. Additionally, when $L_\mathrm{r} >$ 50%, the size reduction ratio is not as large as $L_\mathrm{r} <$ 50%.

In the other approach corresponding to option (B), the size reduction is carried out by replacing conventional FR-4 with high-K material to increase the dielectric constant ε_r of the dielectric layer between the power/ground planes. Taking the wavelength in each medium into account, a size reduction factor, K_r, is given as

$$K_\mathrm{r} = \sqrt{\frac{\varepsilon_\mathrm{r,FR4}}{\varepsilon_\mathrm{r,highK}}}\ (<1), \tag{1}$$

where $\varepsilon_\mathrm{r,FR4}$ and $\varepsilon_\mathrm{r,highK}$ are the dielectric constants of conventional FR-4 and high-K material, respectively. When K_r = 40% is set as the size reduction, the EBG structure with high-K material should be reduced to 40% in size, compared with the EBG structure formed with FR-4.

The two approaches are compatible, and thus they can be carried out simultaneously. Figure 3 plots the transmission coefficient S_{21} measured with a vector network analyzer (VNA) between two ports of the EBG structure with the lattice

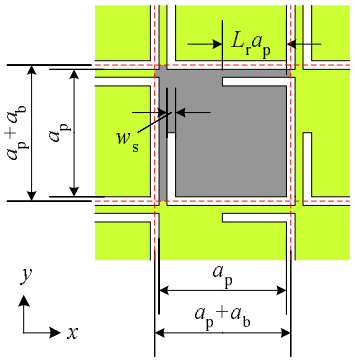

Fig. 2. 2-D unit cells with two narrow slits. Dashed lines indicate the boundary between adjacent unit cells.

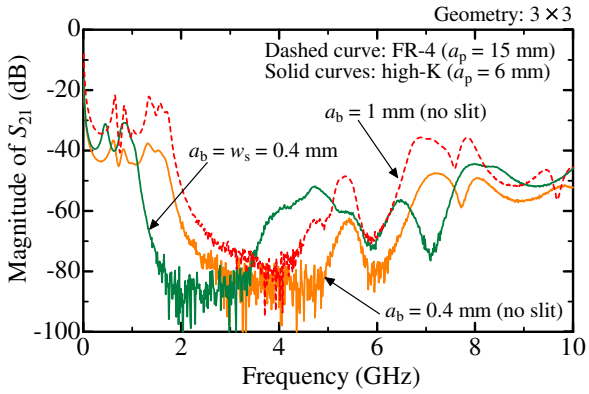

Fig. 3. Stopband shifts towards lower frequencies due to combining the two approaches.

geometry of 3×3, shown in Fig. 1(b). Several test vehicles were fabricated using a high-K material (BC16T, Oak-Mitsui) with ε_{r} = 29.2, $\tan\delta$ = 0.02, and a thickness of 17 μm. The solid curves in Fig 3 indicate the results obtained from the test vehicles with the high-K material. The shift of the fundamental stopband towards the lower frequencies while maintaining high isolation is observed by comparing whether there are slits. Furthermore, a dashed curve indicating a measurement result of the same 3×3 geometry with FR-4, a_{p} = 15 mm, and no slits is included in Fig. 3. This reveals the possibility of size reduction due to the high-K material. As a result, the two approaches were found to be compatible and effective for miniaturization.

C. Miniaturization due to High-permeability Magnetic Materials

The third approach is described in the following section. This approach involves increasing L by using high-permeability magnetic materials, which is associated with option (A). In general, all the materials used for PCBs have unity of relative permeability. Therefore, applying the high-permeability magnetic materials to PCBs is expected to easily increase the total inductance. This paper describes how a commercial EMI suppressor sheet (NEC TOKIN) was used to confirm the effects of the high-permeability magnetic materials.

III. Miniaturization Using High-permeability Magnetic Metal Sheet

A. High-permeability Magnetic Metal Sheet

The commercial EMI suppressor sheet used in the experiments has a large value of relative permeability. The magnetic material used in the noise suppressor sheet usually has complex permeability. The typical characteristics of permeability are plotted in Fig. 4. The real part μ_{r}' exhibits a large value of about 60 or 20. The value of relative permeability decreases with frequency. At the lower frequencies, below 10 MHz, in general, μ_{r}' takes the maximum value, then decreases with frequency and becomes almost unity over 1 GHz. To the contrary, the imaginary part of complex permeability, μ_{r}'', is nearly zero below 10 MHz and increases with frequency. Around a few hundreds of megahertz, μ_{r}'' takes its maximum value. Then, μ_{r}'' keeps the comparatively large value over a wide frequency range.

In the experiments, two types of EMI suppressor sheets were used to investigate the effects of magnetic materials on size reduction. The Type I magnetic material has a higher value than Type II in the real part of relative permeability, μ_{r}'. The properties of the EMI suppressor sheets dealt with in this paper are summarized in Table I.

B. Experimental Approach

To investigate the miniaturization of the EBG structures, several test vehicles of the same 1-D EBG structure with 4×1 geometry, as shown in Fig. 1(a), were fabricated. Table II summarizes the details of the test vehicles used in this study. Various types, thicknesses, and positions of the sheets were used, and they were interposed between the power and ground planes. The test vehicles had a magnetic metal sheet with the same area as the ground plane. Figure 5 illustrates the case where the sheet was sandwiched between the EBG patterned plane and the dielectric. Furthermore, two subminiature-A (SMA) connectors for the VNA measurement were installed, as shown in Fig. 1(a). The dielectric between the power and ground planes was glass-epoxy, and the structural parameters of the unit cell were as follows: a_{p} = 50 mm; a_{b} = 5 mm; d = 1.6 mm.

The size of the patch in the test vehicles used in the experiments was comparatively large. This is because the lower edge frequency of the stopband of the test vehicles was

TABLE I
PROPERTIES OF MAGNETIC METAL SHEETS USED IN THE STUDY.

Type	I	II
Typical μ_{r}' at 1 MHz	60	20
Maximum value of μ_{r}''	20	7
Sheet thickness (mm)	0.1, 0.3	0.3

TABLE II
PROPERTIES OF TEST VEHICLES WITH MAGNETIC METAL SHEETS.

Test vehicle	Type	Thickness (μm)	Position
(i)	I	0.1	EBG pattern-dielectric
(ii)	I	0.1	Dielectric-solid plane
(iii)	I	0.3	EBG pattern-dielectric
(iv)	II	0.3	EBG pattern-dielectric

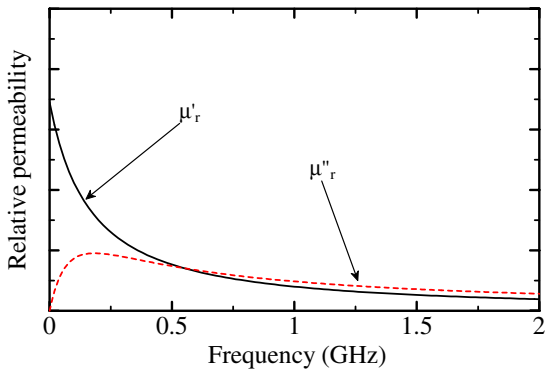

Fig. 4. Typical permeability characteristics of magnetic materials used in this study.

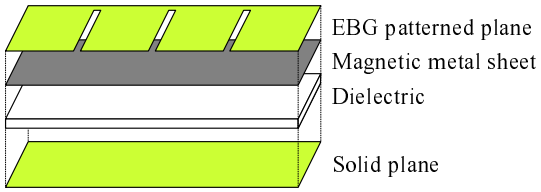

Fig. 5. Insertion of a magnetic metal sheet between the power and ground planes.

set to around 500 MHz, where the relative permeability μ_r' is sufficiently larger than unity.

The solid curves in Fig. 6(a) show the transmission coefficient S_{21} obtained from the two-port VNA measurement. As seen in the figure, the test vehicle, (i), with the interposed magnetic metal sheet has a lower edge frequency of the fundamental stopband than that without the sheet (original). The magnetic metal sheet with high permeability was thus found to be effective for miniaturization.

C. Simulation

To evaluate the effect of complex permeability, a simulation was carried out with a commercial electromagnetic solver, Sonnet. In the simulation, test vehicle (i) was modeled, and then the dielectric constant was set to 4.2 independently of frequency. Regarding the complex permeability of the sheet, μ_r' and μ_r'' are roughly assumed as the solid and dashed lines shown in Fig. 6(b), respectively: $\mu_r' = \mu_r'' = 20$ below 0.8 GHz; $\mu_r' = 20$ and $\mu_r'' = 8$ between 0.8 and 1.6 GHz; and $\mu_r' = 2$ and $\mu_r'' = 3$ above 1.6 GHz. Figure 6(a) plots the transmission coefficient obtained from simulation as well as measurements. As can be seen in the figure, both curves are in good agreement. A wide stopband formed by removing the passband around 1.7 GHz is observed in both the simulation and measurement results. Thus, it was found that the wide stopband results from the imaginary part of complex permeability, μ_r''.

D. Miniaturization effect of magnetic metal sheet

As indicated in Table II, the four test vehicles have slightly different conditions. Using these test vehicles, the differences in miniaturization effects were investigated through measurements.

Figure 7 plots the measurement results of S_{21}. In the figure, the solid curves and dashed curve correspond to the cases with and without a magnetic metal sheet, respectively. For all test vehicles with the magnetic metal sheet, the frequency shift of the fundamental stopband towards the lower frequency is observed. However, the amount of frequency shift depends on the conditions.

First, the largest shift towards the lower frequencies in Fig. 7 results from test vehicle (iii) consisting of the 0.3-mm Type I sheet interposed between the EBG patterned plane and dielectric. The thicker sheet was found to have an efficient effect on the miniaturization.

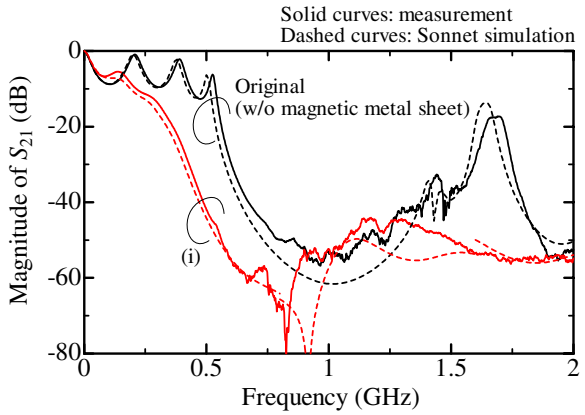

(a) Transmission coefficient of EBG structure with and without magnetic metal sheet.

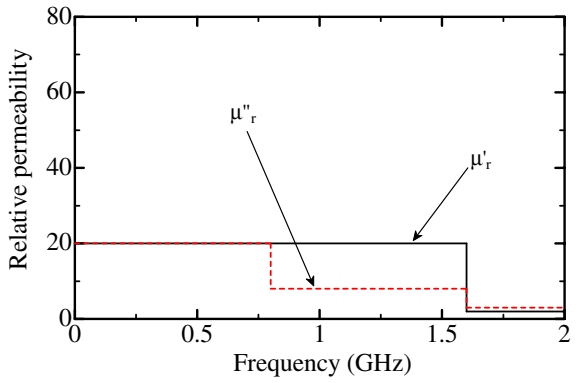

(b) Assumed relative permeabilities as a function of frequency in simulation.

Fig. 6. Comparison of measured and simulated transmission coefficient S_{21} of EBG structure with magnetic metal sheet.

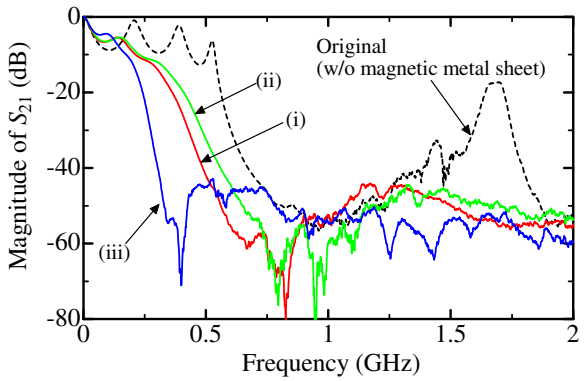

(a) Measured transmission coefficients of EBG structures into which Type I is interposed.

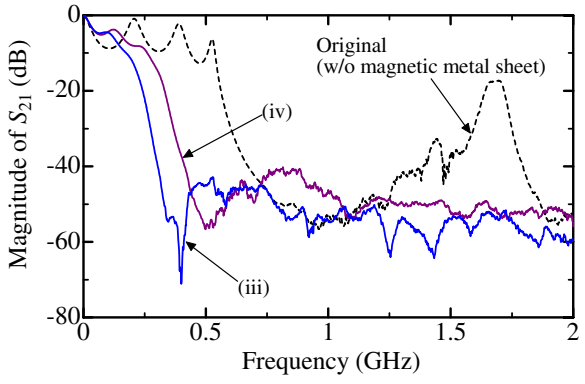

(b) Measured transmission coefficient of EBG structures into which Type I and II are interposed with same thickness.

Fig. 7. Comparison of frequency shifts caused by interposing a magnetic metal sheet.

Next, it is observed in Fig. 7(a) that a magnetic metal sheet placed between the EBG patterned plane and the dielectric shifts the stopband more efficiently than one placed between the dielectric and the ground plane. It is found that the magnetic metal sheet placed on the EBG patterned plane has a greater effect on the inductance of the branch.

Thirdly, higher permeability results in a larger frequency shift, as shown in Fig. 7(b). This result is easily acceptable.

Finally, we again compare the S_{21} characteristics between the cases with and without a magnetic metal sheet. As seen in Fig. 7, no passband around 1.7 GHz and a wide fundamental stopband are observed in all the cases with magnetic metal sheets. The expanded stopband is observed independently of the conditions.

Through the investigations done in this study, miniaturization due to high-permeability magnetic materials was achieved, and the maximum reduction factor in this study was estimated to be approximately 50% through the frequency shift. Because the third approach is compatible with the other two approaches, miniaturization totalling 10% should be achieved by applying all three approaches.

IV. Conclusions

A third approach to miniaturize planar EBG structures formed in a parallel plane pair was investigated. This involves the application of a high-permeability magnetic metal sheet to the parallel plane pair to enlarge the inductance of the EBG unit cell. Through experiments and numerical simulation, this approach was found to be as effective in size reduction as the two previous approaches. In addition, the imaginary part of the permeability was found to contribute to the stopband expansion.

Acknowledgments

The authors would like to thank Dr. Shigeyoshi Yoshida (NEC TOKIN Corporation) and Mr. Kazuhiro Yamazaki (OAK-MITSUI Technologies) for respectively providing the magnetic material sheets and test vehicles with high-K material. The authors are also grateful to Mr. Tasuku Mega, an undergraduate at Okayama University, for his contribution to the experiments.

This research was partially supported by the Grant-in-Aid for Young Scientists (B), No. 18760253, of the Ministry of Education, Culuture, Sports, Science and Technology, Japan.

References

[1] T. E. Moran, K. L. Virga, G. Aguirre, and J. L. Prince, "Methods to Reduce Radiation From Split Ground Planes in RF and Mixed Signal Packaging Structures," *IEEE Trans. Adv. Packag.*, vol. 25, no. 3, pp. 409-416, 2002.

[2] J. Choi, V. Govind, and M. Swaminathan, "A novel electromagnetic bandgap (EBG) structure for mixed-signal system applications," in *Proc. IEEE Radio and Wireless Conf.*, Atlanta, GA, Sep. 2004, pp. 243-246.

[3] J. Choi, V. Govind, M. Swaminathan, L. Wan, and R. Doraiswami, "Isolation in mixed-signal systems using a novel electromagnetic bandgap (EBG) Structure," in *Proc. IEEE 13th Topical Meeting on Electr. Performance of Electron. Packag. (EPEP)*, Portland, OR, Oct. 2004, pp. 199-202.

[4] R. Abhari and G. V. Eleftheriades, "Metallo-dielectric electromagnetic bandgap structures for suppression and isolation of the parallel-plate noise in high-speed circuits," *IEEE Trans. Microw. Theory Tech.*, vol. 51, no. 6, pp. 1629-1639, Jun. 2003.

[5] S. Shahparnia and O. M. Ramahi, "Electromagnetic interference (EMI) reduction from printed circuit boards (PCB) using electromagnetic bandgap structures," *IEEE Trans. Electromagn. Compat.*, vol. 46, no. 4, pp. 580-587, Nov. 2004.

[6] Y. Toyota, A. E. Engin, T. H. Kim, M. Swaminathan, S. Bhattacharya, "Size Reduction of Electromagnetic Bandgap (EBG) Structures with New Geometries and Materials," in *Proc. 56th Electromagn. Compon. Tech. Conf. (ECTC)*, San Diego, CA, May 2006, pp. 1784-1789.

[7] D. M. Pozar, Microwave Engineering, 3rd ed. John Wiley & Sons (New Jersey, 2005), Chap. 8.